Available online at www.sciencedirect.com
SCIENCE DIRECT®
Biochemical Pharmacology 68 (2004) 549–561
Biochemical Pharmacology
www.elsevier.com/locate/biochempharm

Membrane-related effects underlying the biological activity of the anthraquinones emodin and barbaloin

Daiane S. Alves, Laura Pérez-Fons, Amparo Estepa, Vicente Micol*

Instituto de Biología Molecular y Celular, Universidad "Miguel Hernández", Avda. del Ferrocarril s/n. E-03202-Elche, Alicante, Spain

Received 13 February 2004; accepted 21 April 2004

Abstract

Commercial plant extracts containing anthraquinones are being increasingly used for cosmetics, food and pharmaceuticals due to their wide therapeutic and pharmacological properties. In this work, the interaction with model membranes of two representative 1,8-dihydroxyanthraquinones, barbaloin (*Aloe*) and emodin (*Rheum*, *Polygonum*), has been studied in order to explain their effects in biological membranes. Emodin showed a higher affinity for phospholipid membranes than barbaloin did, and was more effective in weakening hydrophobic interactions between hydrocarbon chains in phospholipid bilayers. Whereas emodin induced the formation of hexagonal-H_{II} phase, barbaloin stabilized lamellar structures. Barbaloin promoted the formation of gel–fluid intermediate structures in phosphatidylglycerol membranes at physiological pH and ionic strength values. It is proposed that emodin's chromophore group is located at the upper half of the membrane, whereas barbaloin's one is in a deeper position but having its glucopyranosyl moiety near the phospholipid/water interface. Moreover, membrane disruption by emodin or barbaloin showed specificity for the two major phospholipids present in bacterial membranes, phosphatidylethanolamine and phosphatidylglycerol. In order to relate their strong effects on membranes to their biological activity, the capacity of these compounds to inhibit the infectivity of the viral haemorrhagic septicaemia rhabdovirus (VHSV), a negative RNA enveloped virus, or the growth of *Escherichia coli* was tested. Anthraquinone-loaded liposomes showed a strong antimicrobial activity whereas these compounds in their free form did not. Both anthraquinones showed antiviral activity but only emodin was a virucidal agent. In conclusion, a molecular mechanism based on the effect of these compounds on the structure of biological membranes is proposed to account for their multiple biological activities. Anthraquinone-loaded liposomes may suppose an alternative for antimicrobial, pharmaceutical or cosmetic applications.

Keywords: Anthraquinones; Membrane physical properties; Phosphatidylglycerol; Phosphatidylethanolamine; Antimicrobial; VHSV; Liposomes

1. Introduction

Anthraquinone-containing extracts from different plant sources have been widely used since ancient times due to their laxative and cathartic properties [1]. Besides, this class of compounds have shown a wide variety of pharmacological activities such as anti-inflammatory, wound healing, analgesic, antipyretic, antimicrobial and antitumor activities [2]. Anthraquinones are present in the roots, bark or leaves of numerous plants such as senna, cascara, aloe, frangula and rhubarb.

Barbaloin (10-glucopyranosyl-1,8-dihydroxy-3-(hydroxymethyl)-9(10*H*)-anthracenone: aloin A) (Fig. 1) is the major anthraquinone of *Aloe vera* exudates and gels (*Asphodelaceae*) [3], which are widely used to manufacture several types of beverages, food products, cosmetics and pharmaceuticals. These preparations have shown several pharmacological activities, being laxative the main one [4]. It has been pointed out that cleavage of the glycoside moiety of barbaloin by intestinal flora results in the formation of its aglycon derivate, aloe-emodin, which

Abbreviations: 5-NS, 5-doxyl-stearic acid; 16-NS, 16-doxyl-stearic acid; DAB, diaminobenzidine; DEPE, 1,2-dielaidoyl-*sn*-glycero-3-phosphoethanolamine; DMPC, 1,2-dimyristoyl-*sn*-glycero-3-phosphocholine; DMPG, 1,2-dimyristoyl-*sn*-glycero-3-[phospho-*rac*-(1-glycerol)]; DSC, differential scanning calorimetry; EPC, epithelioma papulosum cyprini cells; FCS, fetal calf serum; H_{II}, inverted hexagonal-H_{II} phase; MIC_{50}, minimal inhibitory concentration corresponding to 50% of cell growth inhibition; K_p, phospholipid/water partition coefficient; LUVs, large unilamellar vesicles; MLVs, multilamellar vesicles; PG, egg yolk phosphatidylglycerol; PE, egg yolk phosphatidylethanolamine; PC, egg yolk phosphatidylcholine; T_c, onset temperature of the gel to liquid-crystalline phase transition; VHSV, viral haemorrhagic septicaemia virus

* Corresponding author. Tel.: +34 966 658430; fax: +34 966 658758.
E-mail address: vmicol@umh.es (V. Micol).

0006-2952/$ – see front matter © 2004 Elsevier Inc. All rights reserved.
doi:10.1016/j.bcp.2004.04.012

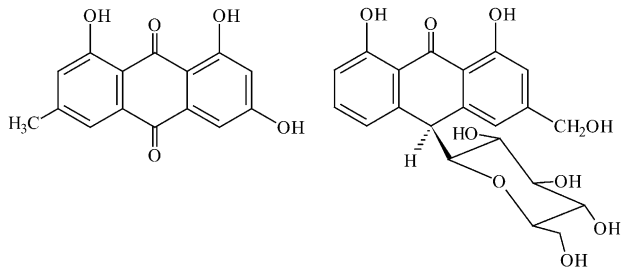

Fig. 1. Chemical structures of the anthraquinones emodin and barbaloin (aloin A).

possesses a stronger laxative effect [5]. Its mechanism is believed to take place through water accumulation in the intestine via active Na^+ transport [6] or by water secretion due to a prostaglandin-dependent mechanism [7]. *Aloe vera* gels and aloins have also dermatological applications based on their capacity to inhibit the activity of microbial and human collagenases and metalloproteases [8,9].

Emodin (1,3,8-trihydroxy-6-methylanthraquinone) (Fig. 1) is the active principle of herbal medicines deriving from genus *Rheum* and *Polygonum* (Polygonaceae), *Rhamnus* (Rhamnaceae) and *Senna* (Cassieae). This anthraquinone has been reported to exhibit anti-inflammatory properties by reduction of cytokine production in human T-lymphocytes and endothelial cells [10,11]. Emodin have also demonstrated antiproliferative effects in several cancer cell lines by promoting apoptosis via caspase-dependent pathways [12,13] or by inhibition of tyrosine protein kinases [14]. Emodin has been recently found to inhibit to protein kinase CK2 [15,16], feature which is suspected to be related to its anticarcinogenic and antiviral activities [17].

1,8-Dihydroxy-anthraquinones have also shown a wide antimicrobial activity. Antibacterial effects of emodin in *Escherichia coli* were proposed to be mediated through inhibition of respiration-driven solute transport in membranes [18]. Other anthraquinones deriving from *A. vera* such as aloe-emodin have also shown effective antibacterial activity at micromolar concentrations, specially for gram-positive bacteria [19,20]. Several anthraquinones, emodin among them, have shown antiviral and/or virucidal activity against enveloped viruses [21–23]. Glycerin *Aloe* extracts and isolated aloe-emodin showed virucidal effects on enveloped viruses such as herpes simplex virus, varicella-zoster virus, pseudorabies virus and influenza virus, most probably by disruption of the virus envelope [23]. In contrast, aloe-emodin was not virucidal against non-enveloped viruses such as adenovirus and rhinovirus. In addition, crysophanic acid (1,8-dihydroxy-3-methylanthraquinone) has demonstrated to inhibit early stages of the replication cycle of non-enveloped viruses such as poliovirus (*Picornaviridae*) [24]. Other anthraquinones such as rhein, emodin, alizarin and quinalizarin exhibited non-virucidal antiviral activity against human cytomegalovirus [25]. Nevertheless, the molecular mechanism of their wide antimicrobial activity is still unknown.

Only in a few cases, anthraquinones pharmacological effects have been directly related to particular cellular events. The multiple biological activities of anthraquinones and their amphiphilic character led us to consider that these compounds may promote complex cellular effects in which perturbation of membrane physical properties might be involved as first events responsible for the subsequent modulation of several enzymes activity. In this work, the molecular interaction of two amphiphilic anthraquinones, emodin and barbaloin, with phospholipids and their effects in the phase behavior of model membranes composed of neutral or negatively charged phospholipids have been studied in order to contribute to the knowledge of their wide biological activity. We have also shown for the first time the use of liposomes as a vehicle to enhance the antimicrobial activity of anthraquinones. In conclusion, this study demonstrates the antimicrobial efficacy of 1,8-dihydroxy-anthraquinones when administered into liposomes as a vehicle system and proposes a membrane-related mechanism to be responsible for their wide biological activity.

2. Materials and methods

2.1. Reagents

1,2-Dimiristoyl-*sn*-glycero-3-phosphocholine (DMPC), 1,2-dielaidoyl-*sn*-glycero-3-phosphoethanolamine (DEPE), 1,2-dimyristoyl-*sn*-glycero-3-[phospho-rac-(1-glycerol)] (DMPG), *E. coli* total lipid extract, L-α-phosphatidylcholine (egg, chicken) (PC), L-α-phosphatidylethanolamine transphosphatidylated (egg, chicken) (PE) and L-α-phosphatidylglycerol (egg, chicken-sodium salt) (PG) were obtained from Avanti Polar Lipids. Stock solutions of these lipids were prepared in chloroform/methanol (1:1) and stored at −20 °C. Phospholipid concentration was determined by the method previously described elsewhere [26]. Spin labels 5-doxyl-stearic acid (5-NS) and 16-doxyl-stearic acid (16-NS), were purchased from Molecular Probes, Inc. Cell culture medium RPMI 1640 Dutch modification was purchased to GIBCO (Invitrogen Corporation). Foetal calf serum (FCS) was obtained from LINUS (Cultek S.L.) and GIEMSA from Sigma-Aldrich Corp. Barbaloin, emodin and 5(6)-carboxyfluorescein (CF) were obtained from Sigma-Aldrich Corp. Anthraquinones stocks were prepared in ethanol and their concentrations were determined using their respective molar absorptivities [emodin: UV (EtOH) λ_{max} 437 nm (log ε 4.1); barbaloin: UV (MeOH) λ_{max} 360 nm (log ε 4.03)].

2.2. Determination of the anthraquinones partition into model membranes

The partition coefficients, K_p, of anthraquinones were calculated from the fluorescence increase of the com-

pounds upon their incorporation into large unilamellar vesicles (LUVs) composed of DMPC, compared with that in the aqueous phase at 30 °C. The phospholipid/water partition coefficient was defined as [27]:

$$K_p = \frac{n_L/V_L}{n_W/V_W} \quad (1)$$

where n_W stands for moles of compound in the aqueous phase (W) and n_L stands for moles of compound in the lipid phase (L), and V for the volume of each phase. To quantify the phospholipid/water partition coefficient, K_p, the following equation was used:

$$\Delta I = \frac{\Delta I_{max}[L]}{1/(K_p\gamma) + [L]'} \quad (2)$$

where ΔI ($\Delta I = I - I_0$) stands for the difference between the fluorescence intensity of emodin and barbaloin measured in the presence (I) and absence of the phospholipid vesicles (I_0); ΔI_{max} ($\Delta I_{max} = I_\infty - I_0$) is the maximum value of this difference once the limiting value is reached (I_∞) upon increasing the phospholipid concentration [L], and γ is the molar volume of the phospholipid (for DMPC in the fluid phase the value of γ is 0.737 M^{-1} [28]).

The concentration of anthraquinones was kept constant (2.6 μM for emodin and 20 μM for barbaloin) and phospholipid concentration was varied. Fluorescence spectra and quenching measurements of anthraquinones were recorded with the SLM-8000C spectrofluorimeter fitted with Glan-Thompson polarizers. Emodin was excited at 430 nm and barbaloin at 395 nm.

2.3. Differential scanning calorimetry

Experiments were performed with a MicroCal MC-2 differential scanning calorimeter interfaced to a computer equipped with a Data Translation DT-2801 A/D converter board for instrument control and automatic data collection. Samples were heated at a constant scan rate of 60 °C/h and held under a constant external pressure of 1 bar. Differences in the heat capacity between the reference and sample cell were obtained by raising the temperature at a constant rate of 1 °C/min over the range from 8 to 37 °C for samples containing DMPC and DMPG and from 20 to 75 °C for samples containing DEPE. Three consecutive scans of the samples were obtained and the second one of the series was analyzed using the software package Origin (Microcal Software, Inc.). Onset (T_c) and completion transition temperatures for the phospholipids were determined as described previously [29].

Samples containing 2.6 μmol of phospholipids (DMPC, DMPG or DEPE) dissolved in chloroform/methanol (1:1) with the corresponding anthraquinones were dried in gaseous N_2 free of oxygen to obtain a film of lipids in a glass tube. To eliminate the last traces of solvent in the samples, they were maintained for 3 h under high vacuum. Multilamellar vesicles (MLVs) were obtained by suspension of the lipid in buffer (10 mM HEPES, 100 mM NaCl, 0.1 mM EDTA, pH 7.4) by vigorous vortexing at a temperature above gel to liquid-crystalline phase transition for DMPC and DMPG (23 °C), but below the temperature of lamellar liquid-crystalline to hexagonal-H_{II} (63 °C) for DEPE. To assure reproducibility in the MLVs preparation samples were frozen and thawed out for three cycles.

2.4. Fluorescence quenching experiments

Fluorescence quenching experiments were carried out using LUVs of DMPC at lipid saturation conditions obtained from the partition curves, by adding aliquots from 1 mM stocks of quenchers in ethanol, at a constant temperature of 30 °C. Differential quenching data using 5-NS and 16-NS were analyzed by Stern–Volmer plot of I_0/I versus $[Q]_L$, where I_0 and I stand for the fluorescence intensity in the absence and in the presence of the quencher respectively; $[Q]_L$ is the spin label quencher concentration given by Eq. (3):

$$[Q]_L = \frac{K_{pQ}V_T}{V_W + V_L K_{pQ}}[Q]_T \quad (3)$$

where $K_{pQ} = [Q]_L/[Q]_W$ is the partition coefficient of the quencher between the phospholipid phase and aqueous phase, respectively, $[Q]_T$ is the concentration of the quencher in the total volume ($V_T = V_L + V_W$), where V_L and V_W are the volume of lipid and aqueous phases. The K_{pQ} for 5-NS and 16-NS are 89,000 and 9730, respectively [30].

2.5. Leakage of intraliposomal carboxyfluorescein

The dried lipids were resuspended in carboxyfluorescein at a concentration of 40 mM in buffer (10 mM Hepes, 100 mM NaCl, 0.1 mM EDTA, pH 7.4). Liposomes (LUVs) were prepared as previously described [31,32]. These were composed of a total lipid extract from *E. coli*. Several mixtures composed of different ratios of phospholipids deriving from egg yolk and having the same acyl chain composition were also used, i.e. PC/PG (1:1), PC/PE (1:1) and PC/PE/PG (4:3:3). CF was encapsulated into liposomes as previously described [33] to monitor the leakage caused by different concentrations of the anthraquinones.

2.6. 90° Light scattering measurements

The measurements of light scattering were done at 280 nm and at temperatures ranging 10–40 °C, in a SLM 8000 spectrofluorometer, interfaced with a Haake water bath. After achieving the desired temperature, the sample was left for at least 5 min at each temperature before the measurement was done. Final lipid concentration in the cuvette was 3 mM.

2.7. Determination of antimicrobial susceptibility

Bacterial growth inhibition was determined using a standard microtiter dilution method in LB no-salt medium (10 g of tryptone and 5 g of yeast extract per liter). Briefly, cells were grown overnight at 37 °C in LB and diluted in the same medium. MICs were determined in triplicate by serial dilutions of anthraquinones-carrying liposomes which were added to the microtiter plates in a volume of 100 μl/well followed by 10 μl of bacteria to give a final inoculum of 5×10^5 CFU/ml. The MIC_{50} was defined as the minimum concentration of anthraquinones that yielded 50% of cell growth inhibition after 26 h incubation. Bacterial growth was determined in a microtiter plate reader by monitoring the OD at 600 nm and was compared to controls in the absence of anthraquinones (100%). To prepare liposomes for antimicrobial activity, anthraquinones were dried together with EYPC from organic solutions and MLVs were prepared as described in Section 2.3. The effect of EYPC liposomes on the antibacterial assay was also determined as a control.

2.8. EPC cell cultures and VHSV

Epithelioma papulosum cyprini (EPC) cell cultures were maintained as previously reported [34]. The virus used to infect fish cells was viral haemorrhagic septicaemia virus VHSV-07.71 [35]. Supernatants from VHSV-07.71 infected EPC cell cultures were clarified by centrifugation at $1000 \times g$ for 20 min and kept in aliquots at −70 °C. Viruses from clarified supernatants were concentrated to 10^{11} foci forming units (ffu)/ml by ultracentrifugation at $100{,}000 \times g$ for 45 min [34].

2.9. Virus infectivity assays

To test the influence of 1,8-dihydroxy-anthraquinones on VHSV infectivity, a previously developed immunostaining focus assay was used [36,37]. Briefly, barbaloin or emodin in aqueous solution or incorporated into EYPC multilamellar vesicles (MLVs) at different molar percentages were incubated with VHSV during 2 h at 4 °C in RPMI-1640 cell culture medium supplemented with 2% fetal calf serum (FCS), 1 mM sodium piruvate, 2 mM L-glutamine, 500 μg/ml gentamicin and 25 μg/ml amphotericin B. The final concentration of phospholipid per well was 0.25 mM. After incubation, the mixtures were added to EPC cell monolayers (200 ffu/well). Alternative treatments were performed consisting of the addition of anthraquinone-loaded liposomes at the infection time or at different times post-infection. Then, the plates were incubated during 24 h at 14 °C. After incubation, cell monolayers were fixed for 10 min in cold methanol and air-dried. Monoclonal antibody (MAb) 2C9 directed towards the N protein of VHSV diluted 1000-fold in dilution buffer (0.24 mM merthiolate, 5 g of Tween 20/l, 50 mg of phenol red/l in PBS pH 6.8) were added to the wells (100 μl/well) and incubated for 90 min at room temperature. After being washed with distilled water, 100 μl of peroxidase-labelled rabbit anti-IgG mouse antibody (Ab) (Nordic) were added per well, and incubation was continued for 45 min. After three washings by immersion in distilled water, 50 μl of 1 mg/ml per well of diaminobenzidine (DAB) (Sigma) in PBS containing H_2O_2 [36,38] were added, and the reaction allowed to proceed until brown foci were detected with an inverted microscope. Once washed with water and air-dried, brown foci (DAB-stained foci) of 15–20 DAB-stained cells or brown cells (DAB-stained single cells) were counted with an inverted microscope (Leica Ltd.) with a 10× ocular eye grid [36]. VHSV titers were expressed as foci forming units per well. Percentage of virus infectivity was calculated by the formula: [(number of foci in the presence of compounds/total number of foci in the absence of compounds) × 100]. Citotoxicity controls were performed by incubating non-infected EPC cells with anthraquinones-carrying liposomes. The effect of EYPC liposomes on the viral infection was also determined as a control.

3. Results

3.1. Anthraquinones membrane affinity

Because of the hydrophobicity of 1,8-dihydroxy-anthraquinones, their interaction with biological membranes may play an important role in order to explain their biological activity. Therefore, the ability of emodin and barbaloin to partition into phospholipid bilayers was tested through the determination of their respective phospholipid/water partition coefficient, K_p, using model membranes. This parameter has higher physiological significance than the regular octanol–water partition coefficient. The increase of the anthraquinones fluorescence intensity observed in the presence of phospholipid vesicles, as compared to that in the aqueous phase, was used to quantify their phospholipid/water partition coefficient, K_p, (Eq. (2)) [27,39] from experiments where phospholipid concentration was varied while anthraquinones concentration was kept constant. The two parameters (ΔI_{max} and K_p) fitting procedure was performed, as described in Section 2, on the experimental data obtained from the enhancement of the anthraquinones fluorescence emission (emodin 560 nm; barbaloin 580 nm) upon addition of LUVs composed of DMPC at 30 °C. K_p values of $(13.93 \pm 2.24) \times 10^3$ and $(1.49 \pm 0.26) \times 10^3$ were obtained for emodin and barbaloin, respectively, which are expected considering that barbaloin is less hydrophobic than emodin due to its glucopyranosyl moiety. However, these values correspond to molecules exhibiting high affinity for phospholipid membranes. Lipid-saturating conditions for fluorescence experiments, i.e. anthraquinones levels associated to membranes ≥92%,

were achieved using millimolar concentrations of lipid versus micromolar concentrations of anthraquinones.

3.2. Effect of anthraquinones on membranes' thermotropic behavior

In order to study the effect of anthraquinones on the thermotropic behavior of phospholipid membranes the technique of differential scanning calorimetry was used. Fig. 2 shows the DSC profiles of DMPC dispersions containing either emodin (Fig. 2A) or barbaloin (Fig. 2B). The presence of increasing amounts of emodin shifted the pretransition of DMPC to lower temperatures. The gel to liquid-crystalline transition ($L_\beta \rightarrow L_\alpha$) phase was also gradually shifted to lower temperatures and its enthalpy decreased as emodin concentration increased from 1 to 5 mol%. At concentrations of 5 mol% of emodin, the onset temperature of the main transition (T_c) was considerably shifted and this transition started to broaden drastically, indicating a strong effect of emodin on the hydrophobic interactions which take place between the hydrocarbon chains of the phospholipids. At concentrations of 15 mol% emodin, the gel to liquid-crystalline phase transition was completely abolished. In contrast, the incorporation of barbaloin into DMPC bilayers had a lighter effect on their thermotropic behavior (Fig. 2B) than that one observed for emodin. The pretransition was slightly shifted to lower temperatures as the concentration of barbaloin increased until 10 mol%, concentration at which this transition disappeared. The main gel to liquid-crystalline phase transition maintained its T_c and enthalpy with no significant changes until 15 mol% barbaloin. Starting at 20 mol%, a decrease of the main transition enthalpy and a broadening was observed but the main transition was still maintained fairly sharp at the highest concentration of barbaloin studied, i.e. 30 mol%.

The effect of the anthraquinones on model membranes composed of DEPE was also studied by DSC (Fig. 3). Aqueous dispersions of DEPE undergo a gel to liquid-crystalline ($L_\beta \rightarrow L_\alpha$) phase transition in the lamellar phase (~37 °C) and, in addition, a lamellar liquid-crystalline to hexagonal-H_{II} ($L_\alpha \rightarrow H_{II}$) transition (~65 °C) [40]. Emodin exhibited a stronger effect than barbaloin on the thermotropic properties of DEPE as it happened to DMPC. The incorporation of emodin into DEPE vesicles started to broaden the gel to liquid-crystalline phase transition at concentrations as low as 1 mol% (Fig. 3A). At concentrations of 2 mol% emodin, a gradual shift of the liquid-crystalline to hexagonal-H_{II} transition to lower temperatures was observed concomitant to the broadening of the main gel to liquid crystalline phase transition. This behavior was maintained up to the highest emodin concentration studied (20 mol%). In addition a new small transition appeared at temperatures below the ($L_\beta \rightarrow L_\alpha$) phase transition, located at approximately 26 °C. In contrast, the incorporation of barbaloin to DEPE dispersions affected the thermotropic behavior of this phospholipid in a less extent. The addition of increasing amounts of barbaloin up to 5 mol% into DEPE (Fig. 3B) slightly affected the gel to liquid-crystalline phase transition and induced a shift of the liquid-crystalline to hexagonal-H_{II} phase to higher temperatures. At concentrations of

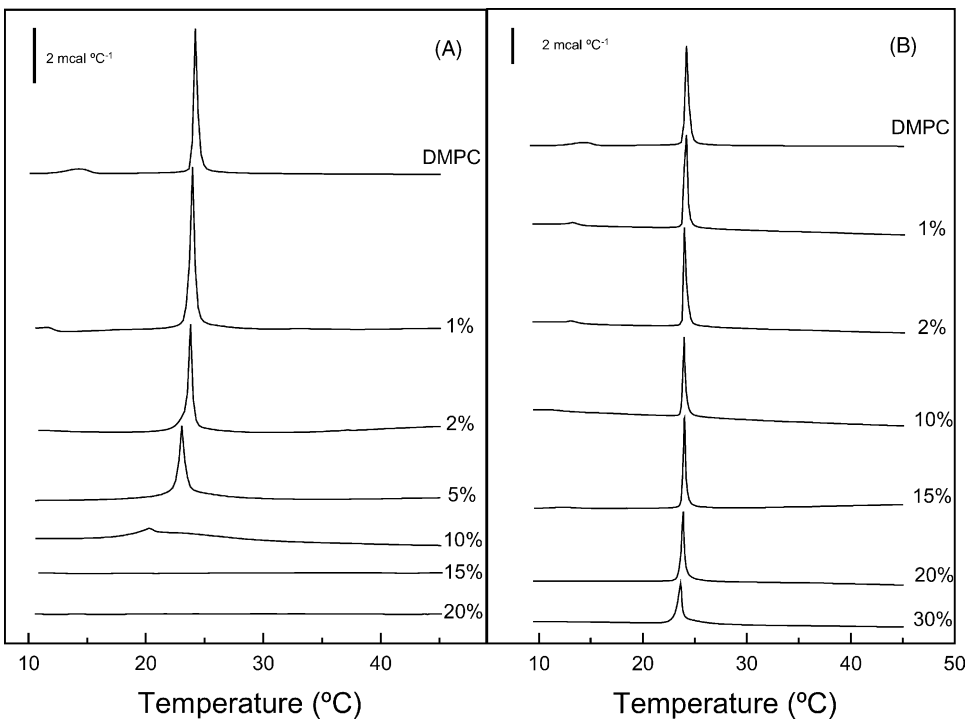

Fig. 2. Differential scanning calorimetry heating thermograms for DMPC lipid dispersions containing emodin (A) or barbaloin (B) at different molar percentages. The concentration of the anthraquinones (molar percentage of total) is indicated on the curves.

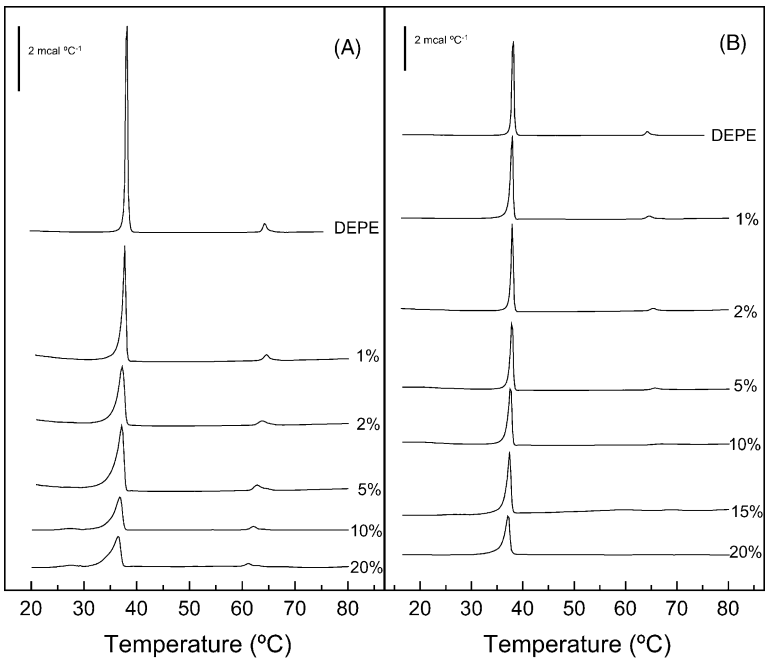

Fig. 3. Differential scanning calorimetry heating thermograms for DEPE lipid dispersions containing emodin (A) or barbaloin (B) at different molar percentages. The concentration of the anthraquinones (molar percentage of total) is indicated on the curves.

10 mol%, the liquid-crystalline to hexagonal-H_{II} phase transition was eliminated and the main phase transition was faintly broadened.

3.3. Formation of gel–fluid phases in phosphatidylglycerol membranes by barbaloin

After studying the effect of emodin or barbaloin on zwiterionic phospholipids such as DMPC or DEPE, the effect on phosphatidylglycerol, a negatively charged phospholipid at physiological pH, was studied. Thermograms corresponding to multilamellar vesicles composed of DMPG and several percentages of the anthraquinones are shown in Fig. 4. The incorporation of emodin to DMPG phospholipid vesicles induced dramatic changes on its thermotropic behavior (Fig. 4A). Concentrations of emodin as low as 1 mol% eliminated the pretransition and induced the formation of a complex DSC profile, showing a

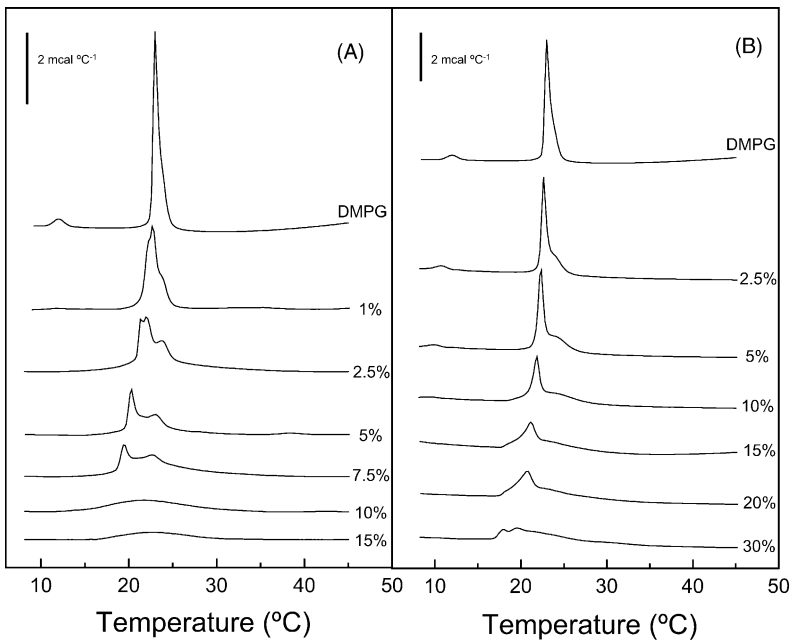

Fig. 4. Differential scanning calorimetry heating thermograms for DMPG lipid dispersions containing emodin (A) or barbaloin (B) at different molar percentages. The concentration of the anthraquinones (mol% of total) is indicated on the curves.

broad gel to liquid-crystalline phase transition with the presence of at least three transition peaks and indicating a lipid phase separation phenomenon. This broad transition decreased its T_c and was observed through 1–7.5 mol% emodin. Starting at 10 mol% emodin, the transition became very broad, fact that was maintained up to 15 mol%, concentration at which the transition was nearly abolished.

On the other hand, barbaloin induced different kind of changes in the thermotropic behavior of DMPG (Fig. 4B). A broad shoulder emerged at temperatures above the gel to liquid-crystalline ($L_\beta \rightarrow L_\alpha$) phase transition meanwhile a sharp transition corresponding to pure phospholipid was concomitant to the broad transition at concentrations of barbaloin as low as 2.5%. This broad transition became broader depending on the increase of barbaloin percentage. The onset temperature of the gel to liquid-crystalline ($L_\beta \rightarrow L_\alpha$) phase transition of DMPG was also shifted to lower temperatures as concentration of barbaloin increased. An identical behavior for DMPG has previously been shown to take place at very low ionic strength [41,42]. Under low salt conditions, DMPG undergoes two phase transitions: one corresponding to the main gel–fluid transition, and a second broad one, called post-transition. Between these two temperatures, structures characterized by low turbidity, high viscosity and high curvature, i.e. extended bilayer networks or gel–fluid intermediates, are postulated [41,43]. This phenomenon is abolished by increasing NaCl or lipid concentrations and osmotically active polymers [41,44]. This particular DSC profile was maintained up to 20 mol% barbaloin. At the highest concentration studied, i.e. 30 mol%, the transition became very broad including several transition peaks.

DMPG gel–fluid phases have also been previously observed through light scattering measurements [42], therefore this technique was used to confirm their presence in DMPG bilayers containing barbaloin. As shown by this technique, DMPG in the presence of 100 mM NaCl undergoes a single sharp transition at 22 °C (Fig. 5A), which corresponds to the gel to liquid-crystalline phase transition. In contrast, at low ionic strength, a sharp decrease of the light scattered at $\theta = 90^\circ$ occurs at the gel to liquid crystalline phase transition, and an increase in the scattering is observed at approximately 30–35 °C corresponding to the post-transition [41,45] (Fig. 5A). The incorporation of barbaloin in DMPG vesicles promoted a light scattering profile more similar to that one shown by this phospholipid at low ionic strength where two transitions were present (Fig. 5B). These profiles exhibited two transitions: one of them corresponding to the onset temperature of the first sharp transition observed by DSC and another transition to higher scattering values matching the broad transition in the DSC profiles, transition that became more intense as barbaloin concentration increased. In contrast, the incorporation of emodin in DMPG bilayers produced a gradual decrease of the light scattered as the temperature was raised, which corresponds to the transition from gel to liquid-crystalline phase (Fig. 5C).

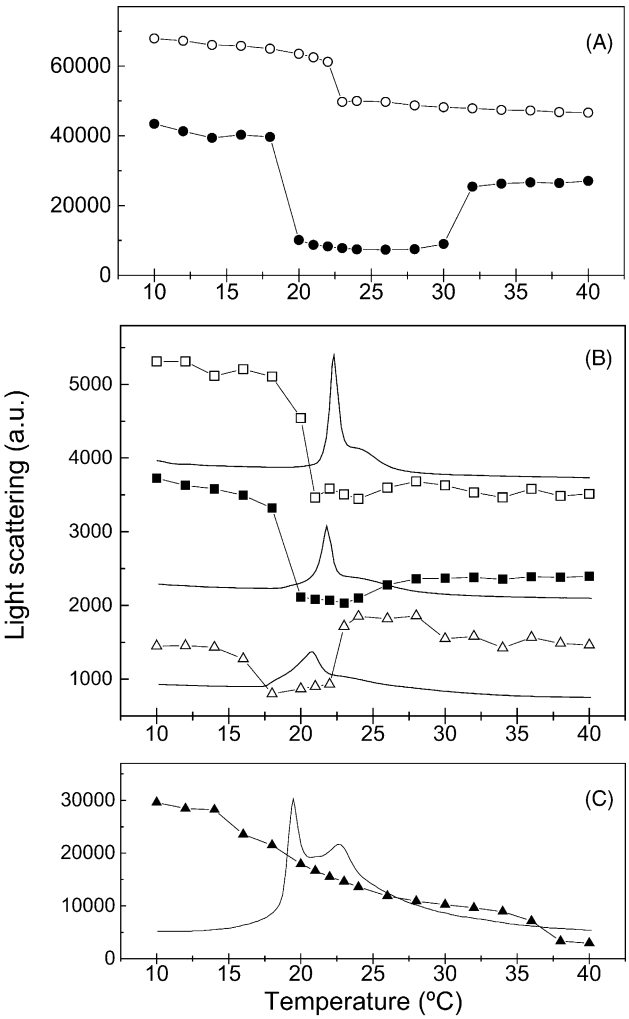

Fig. 5. Effect of barbaloin or emodin on the phase behavior of DMPG membranes. (A) Temperature dependence plots of 90° light scattering ($\lambda = 280$ nm) for pure DMPG dispersions in 100 mM NaCl–HEPES buffer (○) or pure DMPG in the absence of salt (●). (B and C) Differential scanning calorimetry heating thermograms superposed to the temperature dependence plots of 90° light scattering ($\lambda = 280$ nm) corresponding to DMPG dispersions containing different amounts of barbaloin or emodin in 100 mM NaCl–HEPES buffer: 5 mol% barbaloin (□), 10 mol% barbaloin (■), 20 mol% barbaloin (△) or 7.5 mol% emodin (▲). Light scattering curves are the average of three independent measurements.

3.4. Location of anthraquinones in membranes by fluorescence spectroscopy

The transverse penetration of the anthraquinones into the lipid bilayer was investigated by monitoring the relative quenching of its fluorescence by the lipophilic spin probes 5-NS and 16-NS when incorporated into the fluid phase of DMPC vesicles. The Stern–Volmer plots of the fluorescence intensity changes for both anthraquinones are shown in Fig. 6A and B. The probe 5-NS, which has its nitroxide group at carbon-5 region [46], quenched emodin fluorescence more efficiently than 16-NS (Fig. 6A), whereas

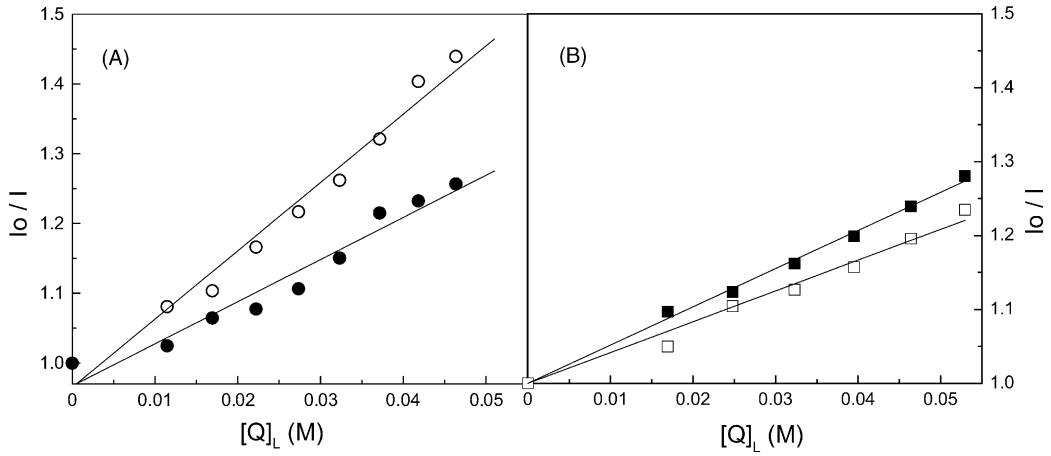

Fig. 6. Stern–Volmer plots for the quenching of emodin or barbaloin fluorescence by spin probes in model membranes. Stern–Volmer plots for the quenching of emodin (A) or barbaloin (B) fluorescence, at a concentration of 30 μM, by 5-NS (open symbols) or 16-NS (closed symbols) and incorporated into LUVs of DMPC at 30 °C at lipid-saturating conditions.

barbaloin seemed to be almost equally quenched by both spin probes (Fig. 6B). These results are compatible with emodin having its cromophore group at the upper part of the phospholipid acyl chains. In contrast, barbaloin's fluorescence was almost equally quenched by both probes, even with a little higher efficacy by 16-NS compared to 5-NS. This result indicates that barbaloin's cromophore group seems to be located in an intermediate position between carbons 5 and 16 at the phospholipid palisade.

3.5. Leakage of liposomes by anthraquinones

In order to detect the capacity of anthraquinones to affect the integrity of phospholipid vesicles through the perturbation of the bilayer, a leakage assay using CF-loaded LUVs composed of synthetic phospholipids bearing identical acyl chain composition (0.8 saturated/unsaturated ratio) and having different head groups was used [39]. Fig. 7A and B show the leakage levels obtained when either emodin or barbaloin were added to phospholipid vesicles composed of PC/PG (1:1), PC/PE (1:1) or PC/PG/PE (4:3:3). Leakage was noticeable at concentrations of emodin > 15 mol% only when PC-model membranes contained PE at a high percentage (50%), and no leakage was observed for vesicles containing PC/PG or a PE content of 33% (Fig. 7A). In contrast, higher levels of leakage were obtained when barbaloin was used (Fig. 7B). Barbaloin promoted a dose-dependent leakage from vesicles composed of PC/PE (1:1), which was significant at low concentrations of this anthraquinone, i.e. 5 mol%. When PC/PG (1:1) model membranes were used, leakage was not noticeable until 15 mol% barbaloin, but starting at this concentration leakage increased steadily to reach a 22% leakage at 30 mol% barbaloin indicating drastic changes in membrane structure. Barbaloin also promoted leakage in model membranes composed of PC/PG/PE (4:3:3). In addition, leakage experiments performed using a total lipid extract from *E. coli* (75% phosphatidylethanolamine, 20% phosphatidylglycerol and 1–5% cardiolipin) were used to detect the perturbation of bacterial membranes by the anthraquinones. As Fig. 7C shows, similar levels of leakage were obtained when anthraquinones concentration was raised to 10 mol%. At concentrations higher than 10 mol%, leakage reached a higher extent in the presence of barbaloin than that one observed when emodin was added.

3.6. Antimicrobial activity of anthraquinone-containing liposomes

Previous studies have demonstrated an antiviral effect of several anthraquinones only when administered in glycerin extracts or in DMSO due to its hydrophobic character [23,24]. Therefore, we studied the efficacy of emodin and barbaloin for antibacterial and/or antiviral activities when incorporated into phospholipid membranes and compared to that one observed in their free form. The antibacterial (bacteriostatic) capacity of emodin and barbaloin was tested by measuring their capability to inhibit the growth of *E. coli* (DH5α). The MIC_{50} was calculated as the lowest anthraquinone concentration at which growth was inhibited at 50% in a broth dilution assay. Anthraquinones were incorporated into MLVs composed of EYPC at a concentration of 20 mol%. Both anthraquinones showed similar MIC_{50} values, 2.2 and 2.8 μM for emodin and barbaloin, respectively. Free compounds were also tested and no growth inhibition was observed at the highest concentration at which both compounds were soluble in culture media, i.e. 15 μM for emodin or 130 μM for barbaloin, as it has been previously observed [47]. Molar percentages of anthraquinones higher than 20% in EYPC MLVs were tested but no higher inhibition was observed.

We also tested emodin or barbaloin for antiviral activity against rhabdoviruses using the viral haemorragic septicaemia virus as a model, a salmonid rhabdovirus, and infecting epithelioma papulosum cyprini (EPC) cell cultures.

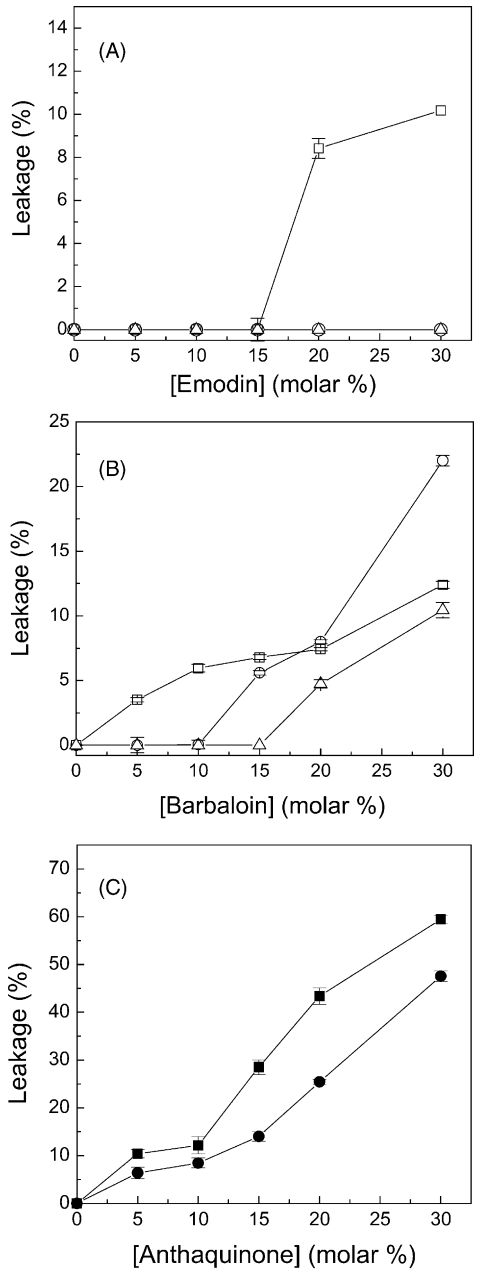

Fig. 7. Leakage of model membranes or *E. coli* membranes in the presence of emodin or barbaloin. Anthraquinone-mediated release from CF-encapsulated liposomes composed of mixtures of egg yolk phospholipids in the presence of increasing concentrations of emodin (A) or barbaloin (B): PC/PG (1:1) (○), PC/PE (1:1) (□) and PC/PE/PG (4:3:3) (△). (C) Anthraquinone-mediated release from CF-encapsulated liposomes composed of a lipid mixture extracted from *E. coli* and containing different molar percentages of emodin (●) or barbaloin (■) at 25 °C. Liposome suspension contained 0.25 mM total phospholipid concentration.

In this case, we did not either detect any capacity for the inhibition of the virus infectivity when the virus was preincubated with these anthraquinones in aqueous solution at concentrations similar to those used in the antibacterial assay. In contrast, EYPC phospholipid vesicles containing emodin or barbaloin inhibited foci formation of VHSV under different conditions. Table 1 shows the percentage of infectivity in VHSV infected EPC cells calculated 24 h post-infection by using several treatments: (i) cell cultures infected with virus preincubated during 2 h with anthraquinone-loaded liposomes, (ii) cells infected with intact VHSV simultaneously to the liposomes addition ($t = 0$), (iii) EPC cells infected with intact VHSV and treated with liposomes added 2 h post-infection, (iv) EPC cells infected with intact VHSV and treated with liposomes added 8 h post-infection (therapeutic effect), and (v) cells incubated with anthraquinone-loaded liposomes for 2 h and then VHSV infected. All treatments used decreased virus microinfectivity in EPC infected cells with a higher efficacy when emodin was used in EYPC vesicles (0–7.5% infectivity) than those in which barbaloin was used (44–92% infectivity), compared to controls of EPC cells treated with intact VHSV (100% infectivity), meaning that emodin was a more efficient antiviral agent than barbaloin under these conditions. Concentrations of the anthraquinones in liposomes higher than 25% were assayed but no further inhibition was detected. In addition, aggregation and precipitation of the liposomes was observed by the microscope at these percentages. No citotoxicity was found for these compounds when incorporated into liposomes at the concentrations assayed.

4. Discussion

1,8-Dihydroxyanthraquinones are active compounds to account for the medicinal and therapeutic properties of many plant-derived drugs. Among their wide biological activity, only in a few cases their molecular mechanism has been elucidated. In this study the interaction of two 1,8-dihydroxyanthraquinones, emodin and barbaloin, with model membranes have been investigated in order to establish the possible role of the effects of these compounds in biological membranes in relation to their pharmacological and therapeutic activities. Both anthraquinones were physically associated to phosphatidylcholine membranes, showing emodin a higher affinity than barbaloin, fact that derives from its higher phospholipid/water partition coefficient. However, both anthraquinones presented high level of association to phospholipid membranes in the conditions used in this work, i.e. lipid-saturating conditions.

Emodin had a much stronger effect than barbaloin on the thermotropic behavior of saturated PC membranes as seen by DSC (Fig. 2). This effect was made manifested by a drastic broadening of the gel to liquid-crystalline phase transition until its disappearance indicating that emodin strongly affects Van der waals interactions between hydrocarbon chains of the phospholipids. A similar effect was observed, although less intense, on the gel to liquid-crystalline phase transition of unsaturated phosphatidylethanolamine membranes (Fig. 3). In addition, emodin shifted the lamellar liquid-crystalline to hexagonal-H_{II} phase

Table 1
VHSV microinfectivity in EPC cell cultures measured 24 h post-infection after different treatments with anthraquinone-loaded EYPC liposomes

Antiviral treatment[a]	Time of treatment (hours)				
	Pre-incubation ($t = -2$)	Infection ($t = 0$)	Post-infection ($t = 2$)	Post-infection ($t = 8$)	Cells treatment + infection ($t = 2$)
25% Barbaloin/EYPC	55.11 ± 3.98	56.95 ± 2.26	44.71 ± 2.19	75.0 ± 9.60	92.0 ± 11.01
25% Emodin/EYPC	6.20 ± 4.38	7.56 ± 4.02	0	0	0

[a] EYPC liposomes containing emodin or barbaloin, at indicated concentrations, were either pre-incubated with VHSV (200 ffu per well of VHSV in 100 μl of medium at 4 °C) for 2 h prior to infection of EPC cell monolayers, added simultaneously at the time of infection ($t = 0$), or added 2 or 8 h post-infection. Alternatively cells were incubated for 2 h and then VHSV-infected. A washing step was included after every treatment. Foci were quantified 24 h post-infection. Results are presented as the percentage of infectivity in the control calculated by the formula: [(number of foci in the presence of compounds/total number of foci in the absence of compounds) × 100]. The data are expressed as the mean ± S.E. of three independent experiments performed in triplicate.

transition allowing the formation of hexagonal phase at lower temperatures compared to pure phospholipid. In contrast, barbaloin only promoted a slight increase of the temperature of this transition. A destabilization of membrane bilayers through the formation of non-bilayer inverted hexagonal (H_{II}) phases is usually promoted by molecules having a hydrophobic volume larger than its polar part (cone-shaped molecules) or molecules which increase the hydrophobic core of the bilayer due to its internal localization. These effects have been previously described for cone-shaped anphipatic molecules such as diacylglycerols [48], or hydrophobic molecules such as vitamin E [49], abietic acid [29] and the antibacterial agents totarol and triclosan [50,51]. Then, the position at which emodin seems to locate at the membrane would induce a higher increase of the hydrophobic part versus the polar region of the membrane therefore promoting non-lamellar phases, such us inverted hexagonal (H_{II}) phase. Since emodin exhibited a higher K_p, the stronger effect of emodin in comparison to barbaloin in phospholipid membranes might be due to its higher effective membrane concentration. Nevertheless, at the conditions used in DSC experiments, effective membrane concentrations were around 94 and 62% for emodin and barbaloin, respectively. This fact leads us to postulate that emodin induces more severe effects than barbaloin does, besides its higher content in membranes.

The results obtained from the fluorescence spectroscopy measurements point out a different location for barbaloin and emodin (Fig. 6A and B). Whereas emodin's chromophore group seems to reside at the upper half of the phospholipid hydrocarbon chains, barbaloin's one might be located at a more internal position, i.e. in a middle-lower position of the phospholipid palisade, but probably having its hydrophilic glucoside moiety closer to the phospholipid/water interface. This scene of the molecules localization would induce the formation of lipid structures more asymmetric in the case of emodin than those when barbaloin is immersed in membranes, which would be responsible for the formation of non-lamellar structures.

We have shown that barbaloin promotes the formation of gel–fluid intermediate structures in phosphatidylglycerol membranes by DSC and light scattering measurements (Fig. 5). Our results indicate that barbaloin is able to produce an effect identical to that one observed for this phospholipid at low ionic strength. These conditions facilitate the formation of lipid structures with high viscosity and curvature due to a lack of cations to stabilize their negatively charged polar groups. This fact leads us to suggest that barbaloin may establish strong molecular interactions with phosphatidylglycerol polar head groups, probably through hydrogen bonding, then shifting Na^+ ions from the membrane surface. This hypothesis is supported by the fact that the behavior shown by DMPG/barbaloin dispersions was reversed by high NaCl concentrations, i.e. 500 mM NaCl or low pH values (pH 5.5), at which DMPG phosphate group was protonated (data not shown), conditions in which gel–fluid structures are also abolished in DMPG vesicles [44].

Leakage experiments yielded that perturbation of phospholipid membranes by anthraquinones showed specificity based on its polar head group. Emodin produced leakage on model membranes composed of phospholipids bearing the same acyl chain composition only when PE was present at a high percentage (≥50%), probably through its capacity to destabilize membranes by the formation of inverted hexagonal-H_{II} phases as it was proven through DSC. This specificity for producing leakage on phosphatidylethanolamine containing membranes has been previously observed for other antibacterial compounds such as galloylated catechins [39]. Considering that phosphatidylethanolamine is the major lipid of the bacterial membrane (as high as 70% of the total phospholipid) [52], the latter effect may account for the antibacterial activity of emodin at least at the membrane level. Nevertheless, other effects on bacterial metabolism cannot be discarded since emodin might be able to easily cross membranes. On the other hand, barbaloin produced a higher level of leakage on *E. coli* membranes than emodin at concentrations of 10 mol% (Fig. 7C). This result was in agreement with those obtained in Fig. 7B, since barbaloin yielded an important leakage when PE was present, but it also produced a significant leakage in the presence of PG, probably involving the promotion of gel–fluid phases, as

demonstrated through DSC and light scattering. These results indicate that it might exist an additive effect of barbaloin on these two phospholipids to account for its capability to perturb *E. coli* membranes. In order to explain the antibacterial activity of anthraquinones, it must also be considered that bacterial membranes contain significant amounts of negatively charged phospholipids such as phosphatidylglycerol and cardiolipin (up to 40 and 5%, respectively) [53], then the effect on these phospholipids could also account for the antibacterial effect of barbaloin, either affecting membrane stability or through the modulation of bacterial membrane proteins activity. In fact, the activity of several membrane-related bacterial enzymes, i.e. signal peptidases, ion channels and K(+)-translocating Kdp kinases is highly dependent on phosphatidylethanolamine and negatively charged phospholipids such as phosphatidylglycerol or cardiolipin [54,55]. The effect of emodin in DMPG membranes was rather different (Fig. 4) and consisted in a drastic lipid phase separation phenomenon. No gel–fluid phases seemed to occur in the presence of emodin as concluded from light scattering measurements (Fig. 5). We must state that although the abovementioned effects of emodin and barbaloin on phosphatidylethanolamine or phosphatidylglycerol membranes have been shown in vitro, these have a biological transcendence since a segregation of these phospholipids into different domains has been recently proven for *E. coli* membranes, showing a proteo-lipid domain being enriched by phosphatidylethanolamine [56].

One of the main findings of the present work is that both anthraquinones showed antimicrobial activity (antiviral or antibacterial) in the studied systems only when they were incorporated into phospholipid model membranes as a vehicle. This fact could have its explanation based on their relative low solubility in aqueous solutions, although barbaloin presented higher solubility than emodin. Emodin or barbaloin, completely solubilized in aqueous solutions at concentrations of 15 or 130 μM, respectively, did not show antimicrobial activity, whereas similar concentrations of these compounds incorporated into liposomes exhibited important antibacterial or antiviral activities.

Regarding the antiviral activity, the higher efficacy of these compounds into the liposomal system must be related to their higher capacity to physically contact viral or cell membranes. Although emodin and barbaloin showed similar antibacterial capacity, the antiviral capacity exhibited by emodin in our system was much higher. In this work it has been demonstrated that both anthraquinones induce dramatic changes in phospholipid membranes although they seem to reside at different locations and exhibit different affinity for membranes. These membrane effects may contribute to the antiviral capacity of both compounds against VHSV through their incorporation into the viral envelope, as it has been shown for aloe-emodin against several enveloped viruses [23], promoting disruption of the viral membrane. Furthermore, the stronger antiviral capacity of emodin could also be based on its ability to inhibit phosphorylation of proteins which are essential for viral life cycle through CK2 inhibition [17]. This would explain why emodin was a very effective antiviral in all treatments, especially when added post-infection or preincubated with cells (Table 1). This assumption would also explicate the higher capacity of barbaloin when preincubated with the virus or in the early stages of the viral cycle (VHSH replication cycle is approximately 6 h), by directly perturbing viral membrane. It might also explicate the lower antiviral capacity of this compound at 2 or 8 h post-infection or when cells were preincubated with barbaloin, because of its lower capacity to be transferred and stay into the cell membrane after the washing step. The higher hydrophobicity of emodin would also contribute to its higher capacity of inhibiting VHSV infectivity through its accumulation in cell membranes after the washing step previous to the infection, as it has been shown for other hydrophobic antivirals [24,57]. Remarkably, emodin must be considered as a virucidal agent since it showed total inhibition against VHSV virus infectivity when added 8 h post-infection (Table 1).

A consideration to take into account regarding the antimicrobial and therapeutic activities of barbaloin (aloin A) is related to its bioavailability. It has been well-established that barbaloin can be partially metabolized to aloe-emodin or aloe-emodin anthrone either by intestinal bacteria [5,58] or in cultured fibroblasts [59]. Therefore, reasonable doubts may arise about whether the antimicrobial activity of barbaloin might be due to the compound itself or to its conversion into aloe-emodin. In our in vitro systems no transformation of barbaloin into aloe-emodin was observed neither in the VHSV-EPC cells system nor in the *E. coli* system (data not shown for briefness), therefore barbaloin antimicrobial activity must be assigned to the compound itself.

In summary, our results indicated that emodin and barbaloin affect dramatically phospholipids membranes and may be responsible for remarkable changes in membrane physical properties. These alterations might consist in changes of the lipid/water interface in negatively charged phospholipids (barbaloin) and perturbations of the core of the bilayer (emodin and barbaloin). Such a diversity of biological effects attributed to 1,8-dihydroxyanthraquinones, i.e. antimicrobial, anticarcinogenic, anti-inflammatory, laxative, vasorelaxant, etc. may be also related to their capacity of modulating membrane physical properties. There are many examples of anthraquinones affecting the activity of membrane-related enzymes or processes such as Ca^{2+} signaling [60], active sodium transport [6], release of inflammatory mediators [61] or platelet-activating factor release into intestine mucose [62]. Furthermore, there are several examples of membrane-related processes regulated by negatively charged phospholipids such as modulation of G-protein-coupled receptors [63], autoimmune diseases, atherosclerosis, and

inflammatory processes [64] or cell signalling, tumorigenesis and inflammation mediated by phospholipase A2 [65].

Some compounds or drugs, as those shown in this work, show a superior therapeutic effect when vehiculized in liposomes as a delivery system due either to a prolonged residence time of the substance, or to a release of the compound at its target site, or to specific interaction (fusion) with its target [66]. This strategy may suppose an important alternative to increase the efficacy of natural anthraquinones for the treatment of microbial infections or other therapeutic applications.

Acknowledgments

This investigation was supported by grants QADVSC2000-70, QADVSC2001-174, CTIDIB/2002/14 and I+D+I2003-GRUPOS03/039 from *Generalitat Valenciana*, and ACU01-003 from INIA (MCyT). We thank Beatriz Bonmatí for her assistance in culture of fish cells and Dr. C. Reyes Mateo for helpful discussion.

References

[1] Thomson RH. Naturally occurring quinones III. Recent advances. London: Chapman and Hall; 1986.
[2] Bisset NG. Herbal drugs and phytopharmaceutical. Boca Ratón: CRC Press; 1994.
[3] Groom QJ, Reynolds T. Barbaloin in aloe species. Planta Med 1986;52:345–8.
[4] Plasket LG. The nature of the plant and its background. In: The health and medical use of *Aloe vera*. Cornwall, UK: Biomedical Information Service Ltd.; 1996. p. 10–7.
[5] Akao T, Che QM, Kobashi K, Hattori M, Namba T. A purgative action of barbaloin is induced by Eubacterium sp. strain BAR, a human intestinal anaerobe, capable of transforming barbaloin to aloe-emodin anthrone. Biol Pharm Bull 1996;19(1):136–8.
[6] Ishii Y, Tanizawa H, Takino Y. Studies of aloe. III. Mechanism of cathartic effect. (2). Chem Pharm Bull (Tokyo) 1990;38(1):197–200.
[7] Capasso F, Mascolo N, Autore G, Duraccio MR. Effect of indomethacin on aloin and 1,8 dioxianthraquinone-induced production of prostaglandins in rat isolated colon. Prostaglandins 1983;26(4): 557–62.
[8] Barrantes E, Guinea M. Inhibition of collagenase and metalloproteinases by aloins and aloe gel. Life Sci 2003;72(7):843–50.
[9] Chithra P, Sajithlal GB, Chandrakasan G. Influence of *Aloe vera* on collagen characteristics in healing dermal wounds in rats. Mol Cell Biochem 1998;181(1/2):71–6.
[10] Kumar A, Dhawan S, Aggarwal BB. Emodin (3-methyl-1,6,8-trihydroxyanthraquinone) inhibits TNF-induced NF-kappaB activation, IkappaB degradation, and expression of cell surface adhesion proteins in human vascular endothelial cells. Oncogene 1998;17(7):913–8.
[11] Kuo YC, Meng HC, Tsai WJ. Regulation of cell proliferation, inflammatory cytokine production and calcium mobilization in primary human T lymphocytes by emodin from *Polygonum hypoleucum* Ohwi. Inflamm Res 2001;50(2):73–82.
[12] Chen YC, Shen SC, Lee WR, Hsu FL, Lin HY, Ko CH, et al. Emodin induces apoptosis in human promyeloleukemic HL-60 cells accompanied by activation of caspase 3 cascade but independent of reactive oxygen species production. Biochem Pharmacol 2002;64(12):1713–24.
[13] Srinivas G, Anto RJ, Srinivas P, Vidhyalakshmi S, Senan VP, Karunagaran D. Emodin induces apoptosis of human cervical cancer cells through poly(ADP-ribose) polymerase cleavage and activation of caspase-9. Eur J Pharmacol 2003;473(2/3):117–25.
[14] Chan TC, Chang CJ, Koonchanok NM, Geahlen RL. Selective inhibition of the growth of ras-transformed human bronchial epithelial cells by emodin, a protein-tyrosine kinase inhibitor. Biochem Biophys Res Commun 1993;193(3):1152–8.
[15] Yim H, Lee YH, Lee CH, Lee SK. Emodin, an anthraquinone derivative isolated from the rhizomes of Rheum palmatum, selectively inhibits the activity of casein kinase II as a competitive inhibitor. Planta Med 1999;65(1):9–13.
[16] Battistutta R, Sarno S, De Moliner E, Papinutto E, Zanotti G, Pinna LA. The replacement of ATP by the competitive inhibitor emodin induces conformational modifications in the catalytic site of protein kinase CK2. J Biol Chem 2000;275(38):29618–22.
[17] Sarno S, Moro S, Meggio F, Zagotto G, Dal Ben D, Ghisellini P, et al. Toward the rational design of protein kinase casein kinase-2 inhibitors. Pharmacol Ther 2002;93(2/3):159–68.
[18] Ubbink-Kok T, Anderson JA, Konings WN. Inhibition of electron transfer and uncoupling effects by emodin and emodinanthrone in Escherichia coli. Antimicrob Agents Chemother 1986;30(1):147–51.
[19] Anke H, Kolthoum I, Zahner H, Laatsch H. Metabolic products of microorganisms. 185. The anthraquinones of the *Aspergillus glaucus* group. I. Occurrence, isolation, identification and antimicrobial activity. Arch Microbiol 1980;126(3):223–30.
[20] Ferro VA, Bradbury F, Cameron P, Shakir E, Rahman SR, Stimson WH. In vitro susceptibility of *Shigella flexneri* and *Streptococcus pyogenes* to inner gel of *Aloe barbadensis* Miller. Antimicrob Agents Chemother 2003;47(3):1137–9.
[21] Cohen PA, Hudson JB, Towers GH. Antiviral activities of anthraquinones, bianthrones and hypericin derivatives from lichens. Experientia 1996;52(2):180–3.
[22] Andersen DO, Weber ND, Wood SG, Hughes BG, Murray BK, North JA. In vitro virucidal activity of selected anthraquinones and anthraquinone derivatives. Antiviral Res 1991;16(2):185–96.
[23] Sydiskis RJ, Owen DG, Lohr JL, Rosler KH, Blomster RN. Inactivation of enveloped viruses by anthraquinones extracted from plants. Antimicrob Agents Chemother 1991;35(12):2463–6.
[24] Semple SJ, Pyke SM, Reynolds GD, Flower RL. In vitro antiviral activity of the anthraquinone chrysophanic acid against poliovirus. Antiviral Res 2001;49(3):169–78.
[25] Barnard DL, Huffman JH, Morris JL, Wood SG, Hughes BG, Sidwell RW. Evaluation of the antiviral activity of anthraquinones, anthrones and anthraquinone derivatives against human cytomegalovirus. Antiviral Res 1992;17(1):63–77.
[26] Böttcher CSJ, Van Gent CM, Priest C. A rapid and sensitive submicro phosphorus determination. Anal Chim Acta 1961;24:203–4.
[27] Mateo CR, Prieto M, Micol V, Shapiro S, Villalain J. A fluorescence study of the interaction and location of (+)-totarol, a diterpenoid bioactive molecule, in model membranes. Biochim Biophys Acta 2000;1509(1/2):167–75.
[28] Marsh D. Handbook of lipid bilayers. Boca Raton, USA: CRC Press; 1990.
[29] Aranda FJ, Villalain J. The interaction of abietic acid with phospholipid membranes. Biochim Biophys Acta 1997;1327(2):171–80.
[30] Wardlaw JR, Sawyer WH, Ghiggino KP. Vertical fluctuations of phospholipid acyl chains in bilayers. FEBS Lett 1987;223(1):20–4.
[31] Mayer LD, Bally MB, Hope MJ, Cullis PR. Techniques for encapsulating bioactive agents into liposomes. Chem Phys Lipids 1986;40(2–4):333–45.
[32] Mayer LD, Hope MJ, Cullis PR. Vesicles of variable sizes produced by a rapid extrusion procedure. Biochim Biophys Acta 1986;858(1):161–8.
[33] Schwarz G, Arbuzova A. Pore kinetics reflected in the dequenching of a lipid vesicle entrapped fluorescent dye. Biochim Biophys Acta 1995;1239(1):51–7.

[34] Basurco B, Coll JM. Spanish isolates and reference strains of viral haemorrhagic septicaemia virus shown similar protein size patterns. Bull Eur Assoc Fish Pathol 1989;9:92–5.
[35] LeBerre M, De Kinkelin P, Metzger A. Identification sérologique des rhabdovirus des salmonidés. Bull Office Int Epizooties 1977;87:391–3.
[36] Lorenzo G, Estepa A, Coll JM. Fast neutralization/immunoperoxidase assay for viral haemorrhagic septicemia with anti-nucleoprotein monoclonal antibody. J Virol Methods 1996;58:1–6.
[37] Perez L, Mas V, Coll J, Estepa A. Enhanced detection of viral hemorrhagic septicemia virus (a salmonid rhabdovirus) by pretreatment of the virus with a combinatorial library-selected peptide. J Virol Methods 2002;106(1):17–23.
[38] Sanz F, Coll JM. Detection of viral haemorrhagic septicemia virus by direct immunoperoxidase with selected anti-nucleoprotein monoclonal antibody. Bull Eur Assoc Fish Pathol 1992;12:116–9.
[39] Caturla N, Vera-Samper E, Villalain J, Mateo CR, Micol V. The relationship between the antioxidant and the antibacterial properties of galloylated catechins and the structure of phospholipid model membranes. Free Radic Biol Med 2003;34(6):648–62.
[40] Gallay J, De Kruijff B. Corticosteroids as effectors of lipid polymorphism of dielaidoylglycerophosphoethanolamine. A study using 31P NMR and differential scanning calorimetry. Eur J Biochem 1984;142(1):105–12.
[41] Heimburg T, Biltonen RL. Thermotropic behavior of dimyristoylphosphatidylglycerol and its interaction with cytochrome *c*. Biochemistry 1994;33(32):9477–88.
[42] Lamy-Freund MT, Riske KA. The peculiar thermo-structural behavior of the anionic lipid DMPG. Chem Phys Lipids 2003;122(1/2):19–32.
[43] Schneider MF, Marsh D, Jahn W, Kloesgen B, Heimburg T. Network formation of lipid membranes: triggering structural transitions by chain melting. Proc Natl Acad Sci USA 1999;96(25):14312–7.
[44] Riske KA, Döbereiner H-G, Lamy-Freund MT. Gel–fluid transitions in dilute versus concentrated DMPG aqueous dispersions. J Phys Chem B 2002;106:239–46.
[45] Riske KA, Politi MJ, Reed WF, Lamy-Freund MT. Temperature and ionic strength dependent light scattering of DMPG dispersions. Chem Phys Lipids 1997;89:31–44.
[46] Ellena JF, Archer SJ, Dominey RN, Hill BD, Cafiso DS. Localizing the nitroxide group of fatty acid and voltage-sensitive spin-labels in phospholipid bilayers. Biochim Biophys Acta 1988;940(1):63–70.
[47] Hatano T, Uebayashi H, Ito H, Shiota S, Tsuchiya T, Yoshida T. Phenolic constituents of Cassia seeds and antibacterial effect of some naphthalenes and anthraquinones on methicillin-resistant Staphylococcus aureus. Chem Pharm Bull (Tokyo) 1999;47(8):1121–7.
[48] Micol V, Aranda FJ, Villalain J, Gomez-Fernandez JC. Effect of diacylglycerols on the HII phase transition of dielaidoyl phosphatidylethanolamine. Biochem Int 1990;20(5):957–65.
[49] Micol V, Aranda FJ, Villalain J, Gomez-Fernandez JC. Influence of Vitamin E on phosphatidylethanolamine lipid polymorphism. Biochim Biophys Acta 1990;1022(2):194–202.
[50] Micol V, Mateo CR, Shapiro S, Aranda FJ, Villalain J. Effects of (+)-totarol, a diterpenoid antibacterial agent, on phospholipid model membranes. Biochim Biophys Acta 2001;1511(2):281–90.
[51] Villalain J, Mateo CR, Aranda FJ, Shapiro S, Micol V. Membranotropic effects of the antibacterial agent Triclosan. Arch Biochem Biophys 2001;390(1):128–36.
[52] van der Does C, Swaving J, van Klompenburg W, Driessen AJ. Non-bilayer lipids stimulate the activity of the reconstituted bacterial protein translocase. J Biol Chem 2000;275(4):2472–8.
[53] Lill R, Dowhan W, Wickner W. The ATPase activity of SecA is regulated by acidic phospholipids, SecY, and the leader and mature domains of precursor proteins. Cell 1990;60(2):271–80.
[54] Stallkamp I, Altendorf K, Jung K. Amino acid replacements in transmembrane domain 1 influence osmosensing but not K+ sensing by the sensor kinase KdpD of *Escherichia coli*. Arch Microbiol 2002;178(6):525–30.
[55] Valiyaveetil FI, Zhou Y, MacKinnon R. Lipids in the structure, folding, and function of the KcsA K+ channel. Biochemistry 2002;41(35):10771–7.
[56] Vanounou S, Parola AH, Fishov I. Phosphatidylethanolamine and phosphatidylglycerol are segregated into different domains in bacterial membrane. A study with pyrene-labelled phospholipids. Mol Microbiol 2003;49(4):1067–79.
[57] Conti C, Genovese D, Santoro R, Stein ML, Orsi N, Fiore L. Activities and mechanisms of action of halogen-substituted flavanoids against poliovirus type 2 infection in vitro. Antimicrob Agents Chemother 1990;34(3):460–6.
[58] Ishii Y, Tanizawa H, Takino Y. Studies of aloe. II. Mechanism of cathartic effect. Yakugaku Zasshi 1988;108(9):904–10.
[59] Wamer WG, Vath P, Falvey DE. In vitro studies on the photobiological properties of aloe emodin and aloin A. Free Radic Biol Med 2003;34(2):233–42.
[60] Ma T, Qi QH, Yang WX, Xu J, Dong ZL. Contractile effects and intracellular Ca2+ signalling induced by emodin in circular smooth muscle cells of rat colon. World J Gastroenterol 2003;9(8):1804–7.
[61] Kai M, Hayashi K, Kaida I, Aki H, Yamamoto M. Permeation-enhancing effect of aloe-emodin anthrone on water-soluble and poorly permeable compounds in rat colonic mucosa. Biol Pharm Bull 2002;25(12):1608–13.
[62] Tavares I, Mascolo N, Izzo AA, Capasso F. Effects of anthraquinone derivatives on PAF release by human gastrointestinal mucosa in vitro. Phytother Res 1996;10:s20–1.
[63] Carman CV, Barak LS, Chen C, Liu-Chen LY, Onorato JJ, Kennedy SP, et al. Mutational analysis of Gbetagamma and phospholipid interaction with G protein-coupled receptor kinase 2. J Biol Chem 2000;275(14):10443–52.
[64] Hammel M, Schwarzenbacher R, Gries A, Kostner GM, Laggner P, Prassl R. Mechanism of the interaction of beta (2)-glycoprotein I with negatively charged phospholipid membranes. Biochemistry 2001; 40(47):14173–81.
[65] Tatulian SA. Toward understanding interfacial activation of secretory phospholipase A2 (PLA2): membrane surface properties and membrane-induced structural changes in the enzyme contribute synergistically to PLA2 activation. Biophys J 2001;80(2):789–800.
[66] Lian T, Ho RJ. Trends and developments in liposome drug delivery systems. J Pharm Sci 2001;90(6):667–80.